Journal of Power Sources 233 (2013) 14–22

Contents lists available at SciVerse ScienceDirect

Journal of Power Sources

journal homepage: www.elsevier.com/locate/jpowsour

Simple algorithms for determining parameters of circuit models for charging/discharging batteries☆

Tingshu Hu*, Hoeguk Jung

Department of Electrical and Computer Engineering, University of Massachusetts, Lowell, MA 01854, USA

HIGHLIGHTS

- ► Simple algorithms are derived for determining circuit models of batteries.
- ► The algorithms rely on solving polynomial equations of special structures.
- ► Analytical solutions to the polynomial equations are derived.
- ► Parameters of the circuit models are extracted from experimental responses.
- ► Experimental and computational results validate the effectiveness of the algorithms.

ARTICLE INFO

Article history:
Received 15 November 2012
Received in revised form
11 January 2013
Accepted 16 January 2013
Available online 28 January 2013

Keywords:
Batteries
Circuit models
Polynomial equations
Linear algebraic equations

ABSTRACT

This paper derives simple algorithms for determining parameters of two circuit models for charging/discharging batteries. The problems of identifying parameters for the circuit models are converted into algebraic problems of solving systems of polynomial equations of special structures. A recent algebraic tool is applied to obtain analytical solutions to these polynomial equations and simple algorithms for extracting model parameters from experimental responses. Computational results are obtained for 3 types of batteries: Li-polymer, lead-acid and NiMH.

1. Introduction

Electrical circuit models have been widely used to describe the charging/discharging dynamics of various types of batteries such as lead-acid, lithium-ion (Li-ion), Li-polymer, nickel metal hydride (NiMH), and fuel cells, e.g., see Refs. [1–24]. As compared with electrochemical models, electrical models are much simpler for computation and simulation. Thus they have been used for analysis, design, and simulation of battery powered electronic systems [1,3,4,6–8,10,23]. They are also important for characterization of battery performance, life-time estimation, power management, and efficient use of batteries [11–15].

There are various types of models for batteries, with varying degrees of complexity, as summarized in Ref. [9]. The Thevenin's equivalent circuit model, as depicted in Fig. 1, is one of the most commonly used model in the literature.

(In some works, such as [25], the independent voltage source is replaced by a controlled voltage source.) The parameters in the model depend on many factors [1,10,14,16], such as SOC, the load, the temperature and even the history of charge and discharge. They can be regarded as constants under a certain working condition and over a relatively short period of time.

An important task in battery modeling is to identify the parameters in the circuit model via some experimental responses. With families of parameters identified for various working conditions, a nonlinear model describing the dependence of these parameters on SOC, current, and temperature, can be obtained with numerical methods. In Ref. [5], we developed a simple analytical method for identifying the parameters for the Thevenin's equivalent circuit model in Fig. 1. Computations show that for 3 different

☆ This work was supported in part by NSF under grants ECCS-0925269, 1200152.
* Corresponding author.
E-mail addresses: tingshu@gmail.com, tingshu_hu@uml.edu (T. Hu), Hoeguk_Jung@student.uml.edu (H. Jung).

0378-7753/$ – see front matter © 2013 Elsevier B.V. All rights reserved.
http://dx.doi.org/10.1016/j.jpowsour.2013.01.098

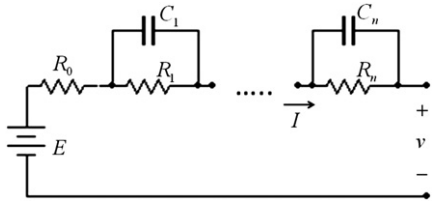

Fig. 1. Circuit model for battery–model I.

types of batteries, the model with two pairs of parallel RCs ($n = 2$) can produce a response that nearly perfectly match the response obtained from experiment. The responses in Ref. [5] were compared for a relatively short time period, e.g., 2 min for a 5 Ah Li-polymer battery. This means that the Thevenin's equivalent model with two pairs of parallel RCs describes the short time transience very well.

A limitation with the model in Fig. 1 (which will be called Model I), is that it is not able to account for the decrease of the open circuit voltage during discharge. This limitation can be addressed by replacing the ideal voltage source with a capacitor C_0 (see Fig. 2) or another pair of parallel resistor R_p and capacitor C_b (see Fig. 3).

These models have also been widely considered in the literature (e.g., see Refs. [2,14]). They will be referred to as Model II and Model III in the sequel. The two models can also be used to describe the charging dynamics and the model in Fig. 3 accounts for the self discharging characteristics. However, it should be noted that each model has a limitation and is only suitable for some working conditions. For instance, they are unable to describe the drop off behavior at the end of discharge or the voltage drop at the end of charging for an NiMH battery.

This paper is a continuation of our recent work [5]. The objective is to derive simple algebraic methods for parameter identification for Model II and Model III. In Ref. [5], we developed an algebraic tool for solving a system of polynomial equations with special structures. This algebraic tool will be extended to determining parameters for Model II and Model III.

2. The algebraic tool

In this section we briefly review the main algebraic tool developed in Ref. [5]. For simplicity of presentation, we consider the following polynomial equations:

$$x_1 + x_2 + x_3 = b_1 \tag{1}$$

$$d_1x_1 + d_2x_2 + d_3x_3 = b_2 \tag{2}$$

$$d_1^2x_1 + d_2^2x_2 + d_3^2x_3 = b_3 \tag{3}$$

$$d_1^3x_1 + d_2^3x_2 + d_3^3x_3 = b_4 \tag{4}$$

$$d_1^4x_1 + d_2^4x_2 + d_3^4x_3 = b_5 \tag{5}$$

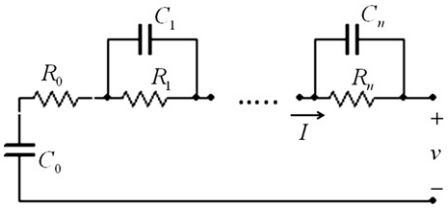

Fig. 2. Circuit model for battery–model II.

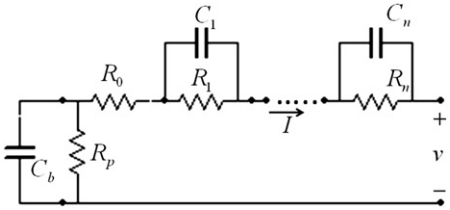

Fig. 3. Circuit model for battery–model III.

$$d_1^5x_1 + d_2^5x_2 + d_3^5x_3 = b_6 \tag{6}$$

where $b_1, b_2,\ldots,b_6$ are given constants and $x_1, x_2, x_3, d_1, d_2, d_3$ are variables to be solved. These equations can be solved by using the following algorithm:

Algorithm I.

1. Compute $\begin{bmatrix} u_1 \\ u_2 \\ u_3 \end{bmatrix} = \begin{bmatrix} b_3 & -b_2 & b_1 \\ b_4 & -b_3 & b_2 \\ b_5 & -b_4 & b_3 \end{bmatrix}^{-1} \begin{bmatrix} b_4 \\ b_5 \\ b_6 \end{bmatrix}$.
2. Let the roots to $q^3 - 2u_1q^2 + (u_1^2 + u_2)q + (u_3 - u_1u_2) = 0$ *be* q_1, q_2, q_3. Then
$$\begin{bmatrix} d_1 \\ d_2 \\ d_3 \end{bmatrix} = \begin{bmatrix} 0 & 1 & 1 \\ 1 & 0 & 1 \\ 1 & 1 & 0 \end{bmatrix}^{-1} \begin{bmatrix} q_1 \\ q_2 \\ q_3 \end{bmatrix}$$
3. Compute $\begin{bmatrix} x_1 \\ x_2 \\ x_3 \end{bmatrix} = \begin{bmatrix} 1 & 1 & 1 \\ d_1 & d_2 & d_3 \\ d_1^2 & d_2^2 & d_3^2 \end{bmatrix}^{-1} \begin{bmatrix} b_1 \\ b_2 \\ b_3 \end{bmatrix}$.

For more general case with $2n$ equations and $2n$ variables x_i, d_i, $i = 1, 2,\ldots,n$, please refer to [5].

3. Algorithm for parameter identification of model II

The model in Fig. 2 can be used to describe both charging and discharging dynamics of a battery. A simple set up to determine the parameters for the charging model is to connect the battery to a constant current source and record the response of the terminal voltage over a period of time. For the discharging model, the battery is connected to a constant current load.

In general, we consider the battery model with n pairs of parallel resistors and capacitors $(R_1, C_1), (R_2, C_2),\ldots,(R_n, C_n)$, as depicted in Fig. 2. Assume that the load (or the current source) is connected at $t = 0$ and that the initial voltages for $C_1, C_2,\ldots,C_n$ are 0. Then the initial voltage for C_0 is the same as the initial terminal voltage of the battery, which is $v(0^-)$. The internal resistance R_0 can be simply obtained from the voltage drop (or rise) at $t = 0$,

$$R_0 = \left(v\left(0^-\right) - v\left(0^+\right)\right)\Big/ I.$$

Note that for discharging, I is positive and for charging, I is negative. The other parameters C_0, (R_1, C_1), …, (R_n, C_n) have to be evaluated via the time response of the voltage $v(t)$ over a period of time.

Since I is a constant, the voltage can be expressed as

$$v(t) = v\left(0^-\right) - \frac{I}{C_0}t - R_0I - \sum_{k=1}^{n} R_kI\left(1 - e^{-\frac{t}{R_kC_k}}\right)$$

As compared with the expression in Ref. [5], which is for the case where C_0 is replaced with an ideal voltage source E, we have an additional term $-I/C_0t$. In the following, we derive explicit formula for computing the parameters by using a voltage response $v(t)$ obtained from experiment.

For simplicity of presentation and without loss of generality, we use a model with three pairs of parallel RCs ($n = 3$) to explain the method. The pattern can be easily extended to more general cases. For the case with $n = 3$,

$$v(t) = v\left(0^-\right) - \frac{I}{C_0}t - R_0 I - R_1 I\left(1 - e^{-\frac{t}{R_1 C_1}}\right) - R_2 I\left(1 - e^{-\frac{t}{R_2 C_2}}\right) - R_3 I\left(1 - e^{-\frac{t}{R_3 C_3}}\right) \tag{7}$$

To find the 7 unknown parameters C_0, (R_k, C_k), $k = 1, 2, 3$, we pick 7 equally spaced time instants, $t_k = kT$, $k = 1,\ldots,7$. Let

$$d_1 = e^{-\frac{T}{R_1 C_1}}, \quad d_2 = e^{-\frac{T}{R_2 C_2}}, \quad d_3 = e^{-\frac{T}{R_3 C_3}}$$

then for $k = 1, 2,\ldots,7$,

$$v(kT) = v\left(0^-\right) - \frac{IT}{C_0}k - R_0 I - R_1 I\left(1 - d_1^k\right) - R_2 I\left(1 - d_2^k\right) - R_3 I\left(1 - d_3^k\right). \tag{8}$$

the first equation for $k = 1$ can be rewritten as

$$\frac{IT}{C_0} + R_1 I(1 - d_1) + R_2 I(1 - d_2) + R_3 I(1 - d_3) = v\left(0^-\right) - v(T) - R_0 I \tag{9}$$

by subtracting $v((k+1)T)$ from $v(kT)$, $k = 1,\ldots,6$ we obtain

$$\frac{IT}{C_0} + R_1 I(1 - d_1)d_1 + R_2 I(1 - d_2)d_2 + R_3 I(1 - d_3)d_3 = v(T) - v(2T) \tag{10}$$

$$\frac{IT}{C_0} + R_1 I(1 - d_1)d_1^2 + R_2 I(1 - d_2)d_2^2 + R_3 I(1 - d_3)d_3^2 = v(2T) - v(3T) \tag{11}$$

$$\vdots$$

$$\frac{IT}{C_0} + R_1 I(1 - d_1)d_1^6 + R_2 I(1 - d_2)d_2^6 + R_3 I(1 - d_3)d_3^6 = v(6T) - v(7T) \tag{12}$$

by subtracting (10) from (9), (11) from (10), and so on, we obtain 6 equations:

$$R_1 I(1 - d_1)^2 + R_2 I(1 - d_2)^2 + R_3 I(1 - d_3)^2 = v\left(0^-\right) - 2v(T) + v(2T) - R_0 I \tag{13}$$

$$R_1 I(1 - d_1)^2 d_1 + R_2 I(1 - d_2)^2 d_2 + R_3 I(1 - d_3)^2 d_3 = v(T) - 2v(2T) + v(3T) \tag{14}$$

$$\vdots$$

$$R_1 I(1 - d_1)^2 d_1^5 + R_2 I(1 - d_2)^2 d_2^5 + R_3 I(1 - d_3)^2 d_3^5 = v(5T) - 2v(6T) + v(7T) \tag{15}$$

by defining

$$x_i = R_i I(1 - d_i)^2, i = 1, 2, 3,$$
$$b_1 = v(0^-) - 2v(T) + v(2T) - R_0 I,$$
$$b_k = v((k-1)T) - 2v(kT) + v((k+1)T),$$
$$k = 2, \ldots, 6,$$

we obtain exactly the same 6 equations as (1)–(6). Thus we can use Algorithm I to find d_k, x_k, $k = 1, 2, 3$. Then compute (R_k,C_k), $k = 1, 2, 3$ from d_k, x_k.

Combining the above arguments and Algorithm I for solving d_k, x_k, $k = 1, 2, 3$ from (1)–(6), we have the following steps for computing the parameters C_0, (R_k, C_k), $k = 1, 2, 3$.

3.1. Steps for computing model II parameters ($n = 3$):

Given a voltage response $v(t)$ under constant charging/discharging current I. Let $R_0 = (v(0^-) - v(0^+))/I$. Choose a time period T and obtain $v(kT)$, $k = 1, 2,\ldots,7$.

1. Compute $b_1 = v(0^-) - 2v(T) + v(2T) - R_0 I$. For $k = 2,\ldots,6$, $b_k = v((k-1)T) - 2v(kT) + v((k+1)T)$.
2. Compute d_k, x_k, $k = 1, 2, 3$ with Algorithm I.
3. Compute $R_k = x_k/I(1 - d_k)^2$, $C_k = -T/R_k \ln(d_k)$, $k = 1, 2, 3$.

Let $x_0 = v\left(0^-\right) - R_0 I - v(T) - R_1 I(1 - d_1) - R_2 I(1 - d_2) - R_3 I(1 - d_3)$.

then $C_0 = TI/x_0$.

For models with n pairs ($n = 2$ or $n > 3$) of parallel RCs, we need to obtain $v(kT)$, $k = 1, 2,\ldots,2n + 1$ and compute b_k, $k = 1, 2,\ldots,2n$ as in step 1. Then use the corresponding algorithm in Ref. [5] to solve d_k, x_k, $k = 1, 2,\ldots,n$. Step 3 is similar except for $k = 1, 2,\ldots,n$.

4. Algorithm for parameter identification of model III

We use the same set up as in Section 3 to identify the parameters for the model depicted in Fig. 3. In fact, we can use the same experimental responses and assume that the load (or the current source) is connected at $t = 0$ and that the initial voltages for C_1, $C_2,\ldots,C_n$ are 0. Then the initial voltage for C_b is the same as the initial terminal voltage of the battery, which is $v(0^-)$. The internal resistance R_0 is also obtained as $R_0 = (v(0^-) - v(0^+))/I$. We need to identify other parameters C_b, R_p, (R_1, C_1),…,(R_n, C_n) via the time response of the voltage $v(t)$ over a period of time.

By the circuit model and the assumption on initial conditions, the terminal voltage can be expressed as

$$v(t) = e^{-\frac{t}{R_p C_b}} v\left(0^-\right) - R_0 I - R_p I\left(1 - e^{-\frac{t}{R_p C_b}}\right) - \sum_{k=1}^{n} R_k I\left(1 - e^{-\frac{t}{R_k C_k}}\right)$$

by adding $v(0^-)$ and subtracting $v(0^-)$, the above can be written as

$$v(t) = v\left(0^-\right) - \left(1 - e^{-\frac{t}{R_p C_b}}\right) v\left(0^-\right) - R_0 I - R_p I\left(1 - e^{-\frac{t}{R_p C_b}}\right) - \sum_{k=1}^{n} R_k I\left(1 - e^{-\frac{t}{R_k C_k}}\right) = v\left(0^-\right) - R_0 I - \left(R_p I + v\left(0^-\right)\right) \times \left(1 - e^{-\frac{t}{R_p C_b}}\right) - \sum_{k=1}^{n} R_k I\left(1 - e^{-\frac{t}{R_k C_k}}\right)$$

for simplicity, we use the model with $n = 2$ to explain the method. In this case

$$v(t) = v\left(0^-\right) - R_0 I - \left(R_p I + v\left(0^-\right)\right)\left(1 - e^{-\frac{t}{R_p C_b}}\right) - R_1 I\left(1 - e^{-\frac{t}{R_1 C_1}}\right) - R_2 I\left(1 - e^{-\frac{t}{R_2 C_2}}\right)$$

to find the 6 unknown parameters C_b, R_p, (R_k, C_k), $k = 1, 2$, we pick 6 equally spaced time instants, $t_k = kT$, $k = 1,\ldots,6$. Let

$$d_1 = e^{-\frac{T}{R_p C_b}}, \quad d_2 = e^{-\frac{T}{R_1 C_1}}, \quad d_3 = e^{-\frac{T}{R_2 C_2}}$$

then for $k = 1, 2,\ldots,6$,

$$v(kT) = v\left(0^-\right) - R_0 I - \left(R_p I + v\left(0^-\right)\right)\left(1 - d_1^k\right) - R_1 I\left(1 - d_2^k\right) - R_2 I\left(1 - d_3^k\right), \quad k = 1, \ldots, 6. \tag{16}$$

define

$$x_1 = \left(R_p I + v\left(0^-\right)\right)(1 - d_1),$$
$$x_2 = R_1 I(1 - d_2),$$
$$x_3 = R_2 I(1 - d_3).$$

the first equation (for $k = 1$) can be written as

$$x_1 + x_2 + x_3 = v\left(0^-\right) - R_0 I - v(T) \tag{17}$$

by subtracting the second from the first, the third from the second, and so on, we obtain 5 other equations

$$d_1^k x_1 + d_2^k x_2 + d_3^k x_3 = v(kT) - v((k+1)T), k = 1, 2, \ldots, 5 \tag{18}$$

If we let $b_1 = v(0^-) - R_0 I - v(T)$, $b_k = v((k-1)T) - v(kT)$, $k = 2$, 3,…,6. Then (17) and (18) yield (1) to (6), which can be solved by Algorithm I.

Combining the above arguments, we have the following steps for computing the parameters C_b, R_p, (R_k, C_k), $k = 1, 2$.

4.1. Steps for computing model III parameters ($n = 2$)

Given a voltage response $v(t)$ under constant charging/discharging current I. Let $R_0 = (v(0^-) - v(0^+))/I$. Choose a time period T and obtain $v(kT)$, $k = 1, 2,\ldots,6$.

1. Compute $b_1 = v(0^-) - R_0 I - v(T)$. For $k = 2,\ldots,6$, $b_k = v((k-1)T) - v(kT)$.
2. Compute d_k, x_k, $k = 1, 2, 3$ with Algorithm I. Re-order the pairs (d_k, x_k), $k = 1, 2, 3$, if necessary, such that $x_1/(1 - d_1) > v(0^-)$.
3. Compute $R_p = x_1/I(1 - d_1) - v(0^-)/I$, $C_b = -T/R_p \ln(d_1)$. For $k = 1$, 2, $R_k = x_{k+1}/I(1 - d_{k+1})$, $C_k = -T/R_k \ln(d_{k+1})$.

Note that in step 2, we may need to re-order the pairs (d_k,x_k), $k = 1, 2, 3$ so that $x_1/(1 - d_1) > v(0^-)$. This is to ensure that R_p computed in step 3 is a positive number. In general, R_1, R_2 are much smaller than R_p and we can re-order (d_k,x_k), $k = 1, 2, 3$ so that $x_1/(1 - d_1)$ is the largest. For Model I or Model II, the order of (d_k,x_k) does not matter.

The above steps can be modified for general cases with $n = 1$, or $n > 2$.

5. Computational results on three batteries

We collected data on charging/discharging responses for 3 batteries: a 6 V lead-acid battery (13 Ah), a 7.2 V NiMH battery (5 Ah) and a 7.4 V Li-polymer battery (5 Ah). A constant current power supply was used to produce the charging responses and a constant current load was used to generate the discharging responses. Terminal voltage responses under constant charging/discharging current were recorded via a 16-digit data acquisition (DAQ) device.

The sampling period of the DAQ was $T_d = 0.1$ s. The input voltage range was −10 V to 10 V. Thus the resolution was $20/2^{16} = 3.0518^{-4}$ V. We also measured the current via a 0.1 Ω resistor to make sure that the current was the set value. No digital or analog filter was used to process the data/signals.

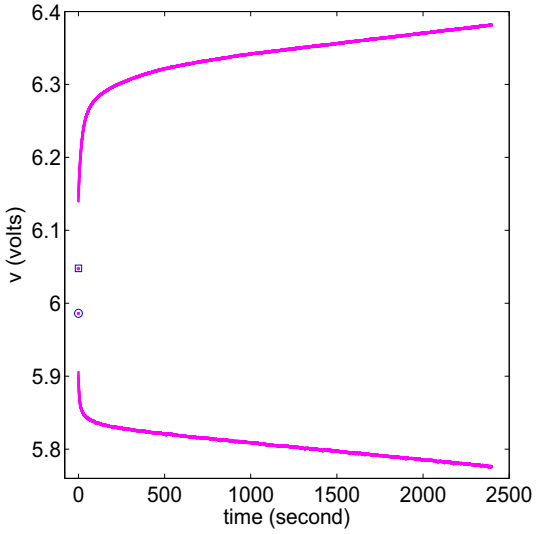

Fig. 4. Charging/discharging terminal voltage response of a lead-acid battery, 1 A, 50% SOC.

All experiment was conducted under room temperature (25 °C).

Unlike a voltage response computed from an analytical expression, the terminal voltage obtained from experiment has various non-idealities. First, the circuit model is only an approximate description of the chemical process inside the battery. Second, the charging/discharging current is not an ideal constant. There are jitterings or ripples around the set value. Third, there are measurement noises and quantization errors. Due to these factors, we did some treatment on the data, as described in Ref. [5]. For instance, we used the average of $v(t)$ around $t = kT$ as $v(kT)$ (the average of a few points may be sufficient). The resulting parameters usually vary with the time period T. We chose T in a certain range so that the root-mean-square-error (RMSE) between the experimental response and the response by the model was minimal. We also used numerical optimization, e.g., "fminsearch", in Matlab, to further reduce the RMSE, by using the parameters obtained using our algorithms as initial values. Note that numerical optimization relies on good initial values.

5.1. Models and responses for a lead-acid battery

The lead-acid battery used for the tests was rated 6 V, 13 Ah. Several charging/discharging cycles were run to collect the data. For each charging/discharging cycle, a fixed current (0.5 A/0.6 A,

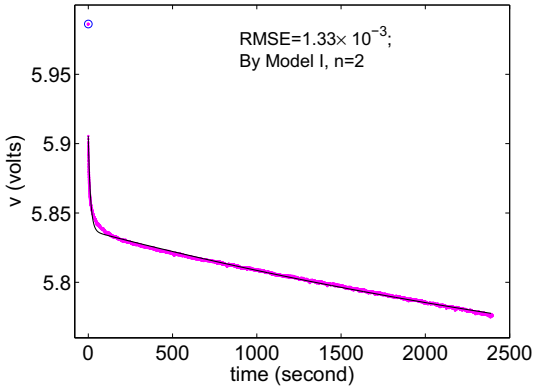

Fig. 5. Discharging response and the response by model I, a lead-acid battery, 1 A, 50% SOC.

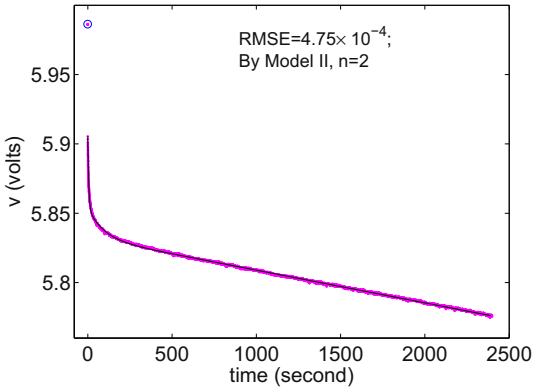

Fig. 6. Discharging response and the response by model II, a lead-acid battery, 1 A, 50% SOCC.

1 A, 1.5 A, 2 A) was used. To examine the dependency of the response on the state of charge (SOC), a charging/discharging cycle was broken down into tests of 40 min, with 40 min of resting period between two tests. (For batteries of smaller or larger capacity, the run time for each test was properly scaled). The number of tests for a charging/discharging cycle and the total time were later used to determine the SOC for each test. For the lead-acid battery under 1 A discharging current, 14 tests were run from fully charged until the sharp drop off.

We first use one discharging test and one charging test to demonstrate the procedure of parameter identification. The charging/discharging current was 1 A (0.077C). Both tests were started at about 50% SOC and lasted 40 min (corresponding to a total of 24,000 points). The two responses are plotted in Fig. 4 for comparison.

For the discharging response, we carried out computation with three models, Model I, Model II and Model III, as depicted in Figs. 1–3, all with $n = 2$. The initial voltage was $v(0^-) = 5.97$ V (see the point marked with "o"), internal resistance $R_0 = 0.0809\ \Omega$.

The parameters for Model I were obtained as follows:

$$R_1 = 0.068\Omega, \quad R_2 = 0.147\Omega, \quad C_1 = 194F,$$
$$C_2 = 3.1 \times 10^4 F$$

The RMSE between the experimental response and the response by the computed model I was 1.33×10^{-3} V.

For Model II,

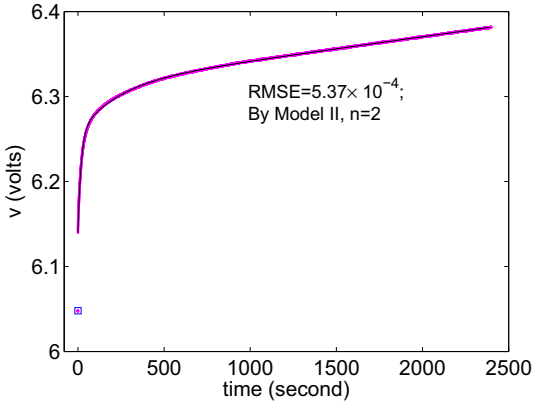

Fig. 7. Charging responses by experimental and new model, 1 A, 50% SOC.

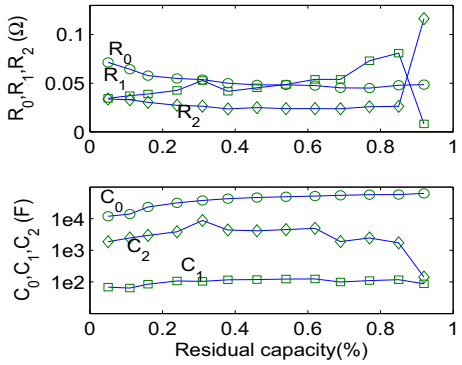

Fig. 8. Model II parameters vs residual capacity, 1 A discharging current.

$$R_1 = 0.0514\Omega, \quad R_2 = 0.0215\Omega,$$
$$C_0 = 4.24 \times 10^4 F, \quad C_1 = 112F, \quad C_2 = 4.25 \times 10^3 F$$

and the RMSE was 4.7489×10^{-4} V.

For Model III

$$R_p = 77.15\Omega, \quad R_1 = 0.0513\Omega, \quad R_2 = 0.0216\Omega,$$
$$C_b = 4.57 \times 10^4 F, \quad C_1 = 111F, \quad C_2 = 4.24 \times 10^3 F$$

and the RMS was 4.7452×10^{-4} V. We see that the parameters of Model II and Model III are very close.

A comparison between the experimental response and the response by model I is shown in Fig. 5, where the experimental response is plotted as the light-colored fuzzy curve and the response by the model is plotted as the thin black curve. There is obvious difference between the two responses for $t < 150$ s. In Ref. [5], we saw that model I could match the initial response (e.g., within the first 2 min) very well, with RMSE $= 8.15 \times 10^{-4}$ V. When it is intended for matching a response for longer period, some mismatch will appear in the initial time. Also, when a different time period is considered, e.g., 10 or 20 min, the resulting parameters will be very different. Clearly, Model I is not suitable for predicting the discharging behavior over a longer time period.

A comparison between the experimental response and the response by model II is shown in Fig. 6. The two responses match nearly perfectly. The thin black curve (model response) lies completely within the light fuzzy curve (experimental response).

The advantage of Model II is that it is able to separate the transient response from the steady decay of the terminal voltage. The time constants of the two parallel RCs are $R_1C_1 = 5.7341$ s,

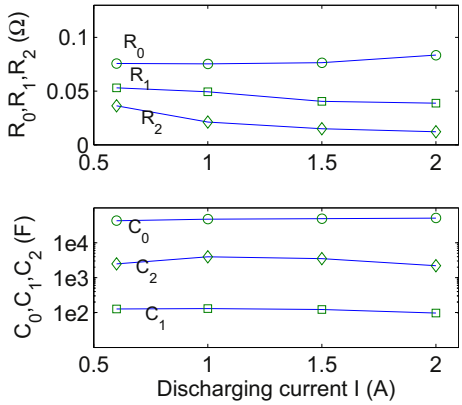

Fig. 9. Model II parameters vs discharging current, 50–70% SOC.

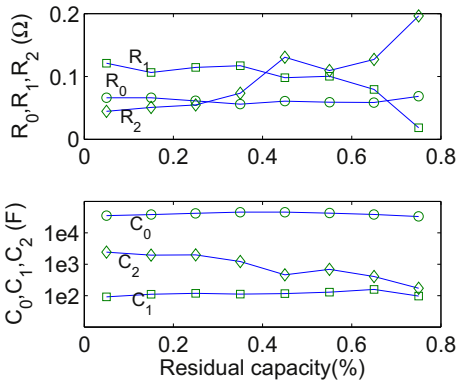

Fig. 10. Model II parameters vs residual capacity, 1.5 A charging current.

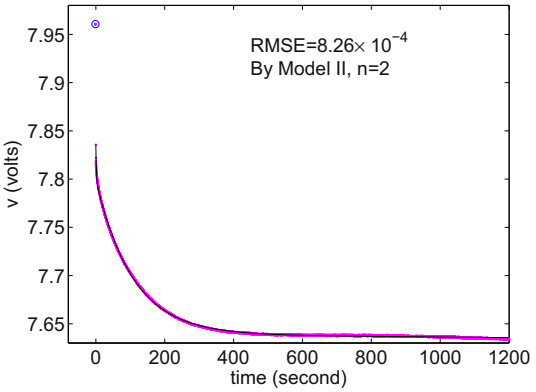

Fig. 12. Discharging responses by experiment and the model, 2 A discharging current, 65% SOC.

$R_2C_2 = 91.48$ s. This shows that the transience vanishes in about $5 \times 91.48 = 457$ s.

The response by Model III was almost the same as that by model II, thus not plotted.

It is interesting to compare the discharging model with the charging model at (approximately) the same SOC. From Fig. 4, it is obvious that the charging response is different from the discharging response in terms of time constants or transient behavior. We would like to know how this difference is reflected by the parameters.

For the charging response in Fig. 4, $v(0^-) = 6.0473$ V (see the point marked with a small box), $R_0 = 0.0907\ \Omega$, the parameters for model I with $n = 2$ were obtained as

$$R_1 = 0.112\Omega, \quad R_2 = 0.14\Omega, \quad C_1 = 1.25 \times 10^4 F, \quad C_2 = 203F$$

The RMSE was 2.7×10^{-3} V. The parameters for Model II were obtained as

$$R_1 = 0.114\Omega, \quad R_2 = 0.056\Omega, \quad C_0 = 3.61 \times 10^4 F, \quad C_1 = 160F, \quad C_2 = 4.01 \times 10^3 F$$

The RMSE was 5.3724×10^{-4} V, which was much improved from Model I. The parameters were different from those of the discharging model but not too far away from them. A comparison of the response by experiment and that by model II is compared in Fig. 7. They match very well.

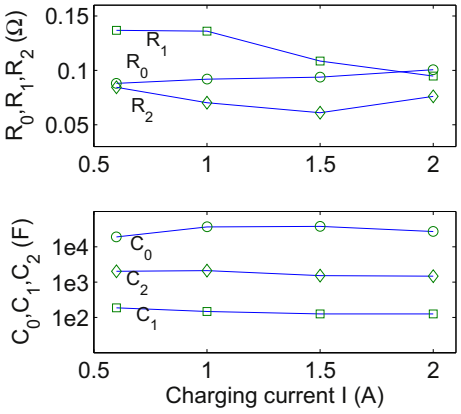

Fig. 11. Model II parameters vs charging current, 50–70% SOC.

The time constants are $R_1C_1 = 18.3189$ s, $R_2C_2 = 225.3208$ s. This confirms that it takes longer for the transience to go away as compared with the discharging process, as shown in Fig. 4.

The parameters for Model III were obtained as:

$$R_p = 82.2\Omega, \quad R_1 = 0.1144\Omega, \quad R_2 = 0.0562\Omega, \quad C_b = 3.34 \times 10^4 F, \quad C_1 = 160F, \quad C_2 = 4.01 \times 10^3 F$$

The RMSE was 5.3709×10^{-4} V, which was very close to that by Model II.

It is known that the parameters depend on factors such as SOC, magnitude of currents and temperature. To obtain a more comprehensive nonlinear model, we can run groups of tests for different charging/discharging current, SOC and/or temperature, and use the method to obtain parameters of the model for the response of every testing condition. Then use numerical methods to obtain a nonlinear function for each parameter with respect to SOC, the current and the temperature. We may also use these parameters identified from experimental responses to validate some nonlinear model derived from theoretical methods.

For some analysis and design purposes, such as robust stability and performance analysis, we need to know the range of each parameter under all possible working conditions. For such purpose, we also need to run groups of tests and identify the parameters for each condition.

Here we use the computational results on several groups of tests to demonstrate some simple relationship between the parameters of Model II and SOC or the current.

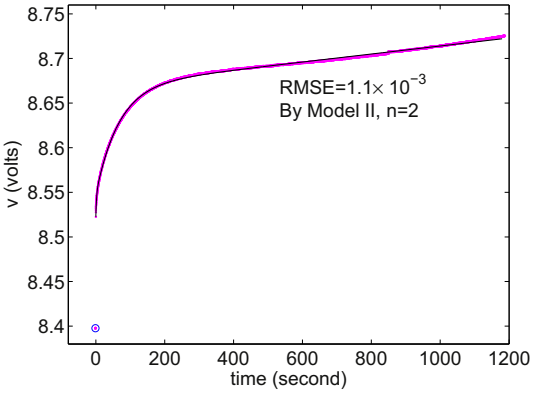

Fig. 13. Responses by experiment and model, 2 A charging current, 55% SOC, NiMH battery.

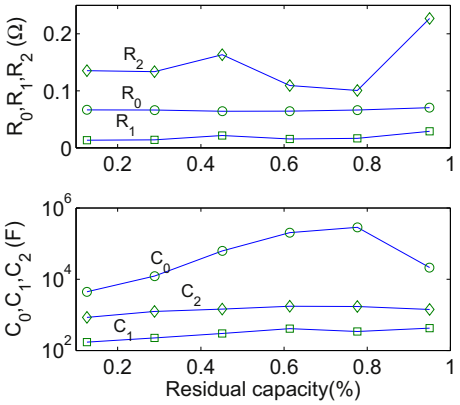

Fig. 14. Discharging parameters vs residual capacity, 1 A discharging current, NiMH battery.

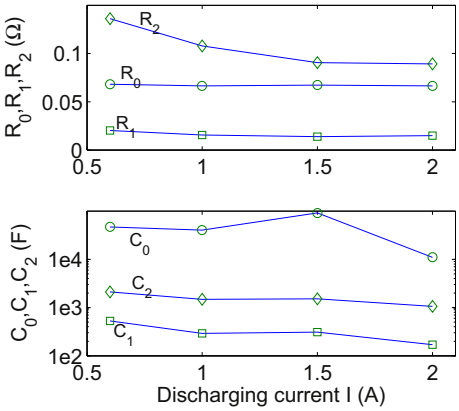

Fig. 16. Discharging parameters vs current, 50–70% SOC, NiMH battery.

Fig. 8 shows the relationship between the parameters and SOC, under 1 A discharging current. We see that between 5% and 85% SOC, there are no significant changes in the parameters except for R_1. Fig. 9 shows the dependence of the parameters on discharging current. The parameters do not change much between 0.6 A and 2 A.

Figs. 10 and 11 show the dependence of the parameters of the charging model on SOC, and charging current, respectively.

5.2. An NIMH battery

The six cell NiMH battery was rated 7.2 V, 5 Ah.

A discharging response (Fig. 12) was obtained at about 65% SOC, with discharging current 2 A (0.4 C). The initial voltage was 7.96 V. Internal resistance $R_0 = 0.0626\ \Omega$.

Three models with $n = 2$ were considered. The parameters for Model I were obtained as follows:

$$R_1 = 0.0803\Omega, R_2 = 0.0192\Omega,$$
$$C_1 = 1394F, C_2 = 100F$$

The RMSE was 0.001 V.

The parameters for model II were obtained as

$$R_1 = 0.0183\Omega, R_2 = 0.0798\Omega,$$
$$C_0 = 6.35 \times 10^5 F, C_1 = 84.9F, C_2 = 1334F$$

The response by experiment and that by Model II are compared in Fig. 12. The two curves overlap very well.

The parameters for Model III were obtained as

$$R_p = 808.3\Omega, R_1 = 0.0183\Omega, R_2 = 0.0798\Omega,$$
$$C_b = 6.38 \times 10^5 F, C_1 = 85F, C_2 = 1334F$$

The RMSE was 8.2613×10^{-4} V.

A charging response was obtained at about 55% SOC, with 2 A charging current. The initial voltage was 8.39 V, internal resistance $R_0 = 0.061\ \Omega$. The parameters for Model II were obtained as follows:

$$R_1 = 0.0123\Omega, \quad R_2 = 0.059\Omega,$$
$$C_0 = 4.566 \times 10^4 F, \quad C_1 = 163F, \quad C_2 = 1130F$$

The charging responses by experiment and by the model are compared in Fig. 13. They overlap well initially but there is some visible difference after 1000 s.

The parameters for Model III were obtained as:

$$R_p = 273\Omega, \quad R_1 = 0.0123\Omega, \quad R_2 = 0.059\Omega$$
$$C_b = 4.5 \times 10^4 F, \quad C_1 = 162F, \quad C_2 = 1131F$$

The RMSE was also 1.1×10^{-3} V.

The dependence of the parameters of discharging models (Model II with $n = 2$) on SOC is plotted in Fig. 14. We see that R_0, R_1, C_1 and C_2 are nearly flat, but there are significant changes in C_0 and R_2. R_2 varies between 0.1005 Ω and 0.2268 Ω, while C_0 varies between $4400F$ and $2.8 \times 10^5 F$. One may wonder if it is still possible to

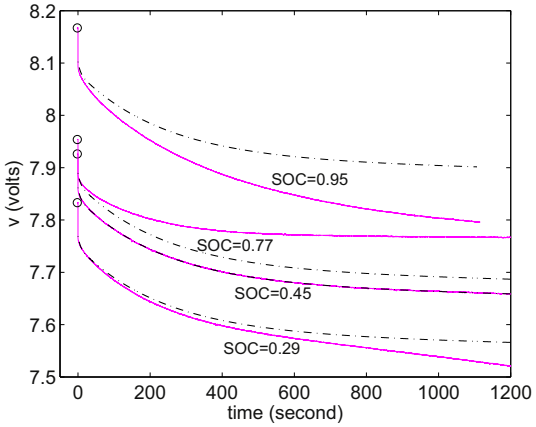

Fig. 15. Using fixed parameters to predict discharging responses for different soc, NiMH battery.

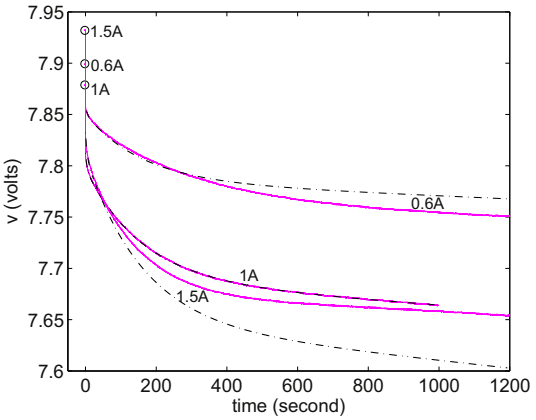

Fig. 17. Using fixed parameters to predict discharging responses for different current, NiMH battery.

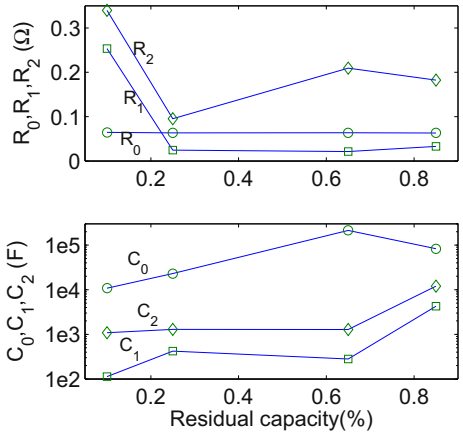

Fig. 18. Charging parameters vs residual capacity, 1.5 A current, NiMH battery.

use a set of fixed parameters to predict the discharging responses over a certain range of SOC, with acceptable errors. Fig. 15 is plotted to show the difference between the predicted response and the measured response for several values of SOC when the parameters obtained for 0.45 SOC are used. In the figure, the predicted responses are plotted with dash-dotted curves and the measured responses with solid curves. The difference between the responses are significant for SOC = 0.77 and 0.95.

The dependence of the parameters of discharging models on the current is plotted in Fig. 16. There are also visible changes in R_2 and C_0, while the other parameters are nearly flat. Fig. 17 is plotted to show the difference between the predicted response and the measured response for several values of discharging current when the parameters obtained for $I = 1$ A are used. The difference is significant for $I = 1.5$ A.

The dependence of the parameters of charging models on SOC is plotted in Fig. 18. All the parameters have significant changes except for R_0. The parameters obtained for 0.65 SOC are used to predict the responses for other values of SOC. The comparison between the predicted response and the measured response is shown in Fig. 19. The prediction errors are significant for both 0.25 SOC and 0.85 SOC.

The dependence of the parameters of charging models on the current are plotted in Fig.20. When a set of fixed parameters are used for predicting the responses under different charging current, there are also significant errors.

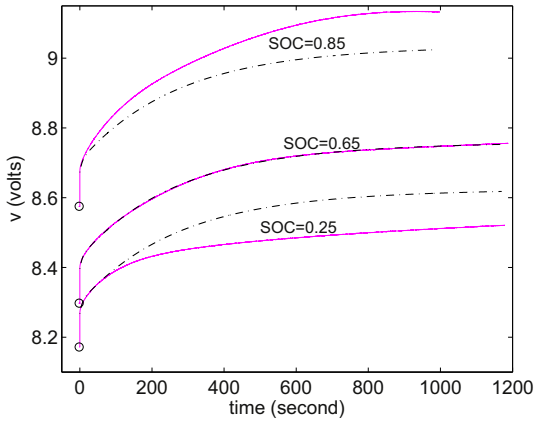

Fig. 19. Using fixed parameters to predict charging responses for different soc, NiMH battery.

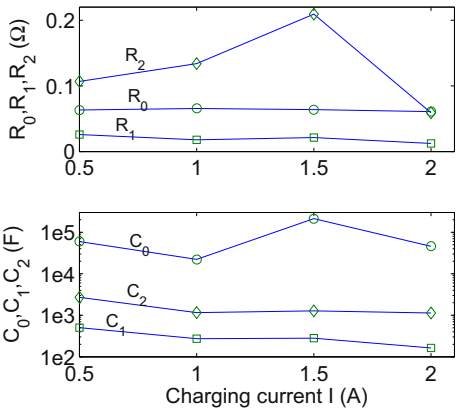

Fig. 20. Parameters vs charging current, 50–70% SOC.

5.3. A Li-polymer battery

The Li-polymer battery had two cells and was rated 7.4 V, 5 Ah. The discharging and charging responses were obtained at about 70% SOC. The charging/discharging currents were 1.5 A (0.3C). For the discharging response, the initial voltage was 7.8055 V and internal resistance $R_0 = 0.0106\ \Omega$. The parameters for Model I were obtained as

$$R_1 = 0.1608\Omega, \quad R_2 = 0.0113\Omega,$$
$$C_1 = 1.2 \times 10^4 F, \quad C_2 = 1228F$$

The RMSE was 3.02×10^{-4} V. The parameters for Model II were obtained as

$$R_1 = 0.0103\Omega, \quad R_2 = 0.0096\Omega,$$
$$C_0 = 1.72 \times 10^4 F, \quad C_1 = 1126F, \quad C_2 = 2.69 \times 10^4 F$$

The discharging response by experiment and that by the model are plotted in Fig. 21. The two responses overlap perfectly. The RMSE was only 2.5172×10^{-4} V, less than the resolution 3.0518×10^{-4} V (the average quantization error is about half of the resolution.)

The parameters for Model III were obtained as

$$R_p = 99.9578\Omega, \quad R_1 = 0.0103\Omega, \quad R_2 = 0.0096\Omega$$
$$C_b = 1.806 \times 10^4 F, \quad C_1 = 1126F, \quad C_2 = 2.692 \times 10^4 F$$

The RMSE was 2.5171×10^{-4} V.

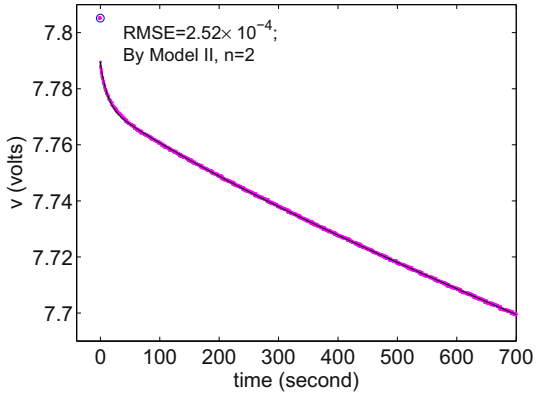

Fig. 21. Discharging responses by experiment and model, 1.5 A current, 70% SOC, a Li-polymer battery.

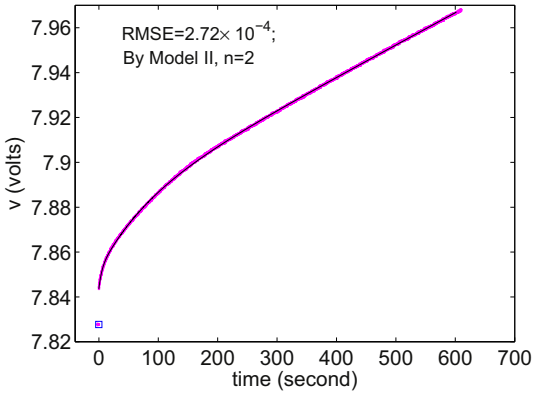

Fig. 22. Charging responses by experiment and model, 1.5 A charging current, 70% SOC.

For the charging response, the initial voltage was 7.8277 V, $R_0 = 0.0106\ \Omega$. The parameters for Model I are,

$$R_1 = 0.1893\Omega, \quad R_2 = 0.0175\Omega, \quad C_1 = 7669F, \quad C_2 = 1973F$$

The RMSE was 8.09×10^{-4} V.

The parameters for Model II,

$$R_1 = 0.0055\Omega, \quad R_2 = 0.019\Omega, \quad C_0 = 1.044 \times 10^4 F, \quad C_1 = 863F, \quad C_2 = 4211F$$

The charging response by experiment and that by the model are plotted in Fig. 22.

The parameters for the charging and discharging models are very different, especially C_2.

For Model III,

$$R_p = 106.5\Omega, \quad R_1 = 0.0055\Omega, \quad R_2 = 0.0191\Omega, \quad C_b = 9925F, \quad C_1 = 863F, \quad C_2 = 4210F$$

The RMSE was 2.7174×10^{-4} V.

Figures were plotted for the dependence of the parameters on SOC or current but not included since they are not very different than those for the other two batteries.

6. Conclusions

We derived simple algorithms for determining parameters of two circuit models for batteries. An algebraic tool for solving a system of polynomial equations was applied to extract the parameters from experimental responses. Several examples demonstrate the effectiveness of the algorithms.

A limitation with the algorithms is the assumption that the battery is in a rested state before each charging/discharging test. This requires a sufficiently long resting time between two tests and will slow down the process of parameter evaluation. It also makes the algorithms inapplicable when the battery is in operation. In our future study, we will try to derive improved algorithms which are able to identify both the initial conditions of the capacitor voltages and the parameters. Preliminary investigation shows that the initial conditions cannot be separated from the parameters if a constant current is applied, and using a current switching between two values may provide a solution.

References

[1] M. Ceraolo, New dynamical models of lead-acid batteries, IEEE Trans. Power Syst. 15 (4) (2000) 1184–1190.
[2] M.A. Cassaca, Z.M. Salameh, Determination of lead-acid battery capacity via mathematical modeling techniques, IEEE Trans. Energy Convers. 7 (3) (1992) 442–444.
[3] S.X. Chen, K.J. Tseng, S.S. Choi, Modeling of Lithium-ion Battery for Energy Storage System Simulation, Power and energy engineering conference, 2009, p. 1–4.
[4] L. Gao, S. Liu, R.A. Dougal, Dynamic lithium-ion battery model for system simulation, IEEE Trans. Compon. Pack. Tech. 25 (3) (2002) 495–505.
[5] T. Hu, B. Zanchi, J. Zhao, Simple analytical method for determining parameters of discharging batteries, IEEE Trans. Energy Convers. 26 (3) (2011) 787–798.
[6] R.C. Kroeze, P.T. Krein, Electrical Battery Model for Use in Dynamic Electric Vehicle Simulations, IEEE conference on power electronics specialists, 2008, p. 1336–1342.
[7] M. Palma, P. Harfman-Todorovic, S. Choi Enjeti, Analysis of DC-dc Converter Stability in Fuel Cell Powered Portable Electronic Systems, 37th IEEE Power electronics specialists conference, June 2006, p. 1–6.
[8] C. Speltino, D. Di Domenico, G. Fiengo, A. Stefanopoulou, Comparison of Reduced Order Lithium-ion Battery Models for Control Applications, Joint 48th IEEE Conf. on Deci. and Contr. and 28th Chinese Contr. Conf, 2009, p. 3276–3281.
[9] K. Sun, Q. Shu, Overview of the Types of Battery Models. Proc. of the 30th Chinese Control Conference (CCC), July 2011, p. 3644–3648.
[10] S. Tian, M. Hong, M. Ouyang, An experimental study and nonlinear modeling of discharge IV behavior of valve-regulated leadacid batteries, IEEE Trans. Energy Convers. 24 (2) (2009) 452–458.
[11] L. Benini, G. Castelli, A. Macii, E. Macii, M. Poncino, R. Scarsi, A Discrete-time Battery Model for High-level Power Estimation, Proc. of the Conf. on Design, Automat. and Test in Europe, 2000, p. 35–41.
[12] M. Durr, A. Cruden, S. Gair, J.R. McDonald, Dynamic model of a lead acid battery for use in a domestic fuel cell system, J. Power Sources 161 (2) (2006) 1400–1411.
[13] J.F.A. Leao, L.V. Hartmann, M.B.R. Correa, A.M.N. Lima, Lead-acid Battery Modeling and SOC Monitoring, Applied Power Electronics Conference and Exposition (APEC), 2010, p. 239–243.
[14] Z.M. Salameh, M.A. Casacca, W.A. Lynch, A mathematical model for lead-acid batteries, IEEE Trans. Energy Convers. 7 (1) (1992) 93–98.
[15] J. Zhang, C. Song, H. Sharif, M. Alahmad, An Enhanced Circuit-based Model for Single-cell Battery, Applied power electronics conference and exposition, 2010 Twenty-Fifth Annual IEEE, 2010, p. 672–675.
[16] S. Barsali, M. Ceraolo, Dynamical Models of Lead-Acid Batteries: Implementation Issues, IEEE Trans. Energy Convers. 17 (1) (2002) 16–23.
[17] H.-C. Chang, C.-M. Liaw, On the front-end converter and its control for a battery powered switched-reluctance motor drive, IEEE Trans. Power Electron. 23 (4) (2008) 2143–2156.
[18] N. Jantharamin, L. Zhang, A New Dynamic Model for Lead-acid Batteries, IET Conf. on Power Electronics, Machines and Drives, 2008, p. 86–90.
[19] G. Livint, M. Ratoi, V. Horga, M. Albu, Estimation of battery parameters based on continuous-time model, Int. Symp. Signals Circuits Systems 2 (2007) 1–4.
[20] D.D.-C. Lu, V.G. Agelidis, Photovoltaic-battery-powered DC bus system for common porftable electronic devices, IEEE Trans. Power Electron. 24 (3) (2009) 849–855.
[21] N. Moubayed, J. Kouta, A. El-Ali, H. Dernayka, R. Outbib, Parameter Identification of the Lead-acid Battery Model, Photovoltaic specialists conference, 2008, p. 1–6.
[22] C. Wang, M.H. Nehrir, S.R. Shaw, Dynamic models and model validation for PEM fuel cells using electrical circuits, IEEE Trans. Energy Convers. 20 (2) (2005) 442–451.
[23] Y. Yao, F. Fassinou, T. Hu, Stability and robust regulation of battery driven boost converter with simple feedback, IEEE Trans. Power Electron. 26 (9) (Sept. 2011) 2614–2626.
[24] J. Zhang, C. Song, H. Sharif, M. Alahmad, Modeling discharge behavior of multicell battery, IEEE Trans. Energy Convers. 25 (4) (2010) 1133–1141.
[25] M. Chen, G.A. Rincon-Mora, Accurate electrical battery model capable of predicting runtime and I-V performance, IEEE Trans. Energy Convers. 21 (2) (2006) 504–511.